Clustering, grouping, self-induced switching, and controlled dynamic pattern generation in an antiphase intracavity second-harmonic-generation laser

Kenju Otsuka and Yoshinori Sato
Department of Applied Physics, Tokai University, 1117 Kitakaname, Hiratsuka, Kanagawa, 259-12 Japan

Jyh-Long Chern
Department of Physics, National Chung Kung University, Tainan, 70101 Republic of China
(Received 11 March 1997)

Antiphase dynamics in globally coupled optical systems are investigated numerically in the model of intracavity second-harmonic generation in multimode lasers. Clustering, grouping of antiphase motions, and self-induced chaotic switching among a factorial number of coexisting grouping states, leading to antiphase periodic states, are found to occur when a pump parameter is increased. Dynamical characterization of grouping behavior and self-induced switching is carried out by global intensity circulation analysis. Nonreciprocal independence of intensity flow in grouping states and switching-path formation process among coexisting grouping states are presented. The controlled switching-path formation between different periodic grouping states by perturbation-pulse injections is demonstrated. [S1063-651X(97)00910-0]

PACS number(s): 42.50.Ar, 02.90.+p, 05.45.+b

I. INTRODUCTION

Antiphase dynamics in globally coupled nonlinear oscillator systems is one of the intriguing issues in complex systems. Antiphase periodic states have been investigated experimentally and theoretically in such systems as coupled Josephson junction oscillators [1], coupled chemical oscillators [2,3], intracavity second-harmonic generation in multimode lasers [4], and modulated multimode lasers and laser arrays [5,6]. Similar spatiotemporal electroencephalogram (EEG) pattern generations have been reported in olfactory sensing systems [7]. In laser systems, novel phenomena associated with antiphase periodic states (abbreviated APS) including injection-seeded factorial dynamic memory [5,6], grouping of antiphase motions leading to cooperatively synchronized chaos [8], as well as chaotic itinerancy among ruins of local APS chaotic attractors in the destruction process of APS's [9] have been reported.

In this paper, several dynamical behaviors associated with Q-switching-type APS's have been found in the model of intracavity second-harmonic generation in multimode lasers in the regime of highly efficient conversion into the second harmonic. They include clustering, grouping in antiphase oscillations, self-induced chaotic switching among coexisting grouping states, and intermittent chaotic antiphase motion in high-dimensional phase space. Dynamical characterization of the grouping state has been carried out in terms of circulation analysis [10,11]. Nonreciprocal independence of intensity flow in grouping states and switching-path formation process among a factorial number of coexisting grouping states have been identified numerically. ''Timing''-controlled perturbation-pulse-induced flexible successive dynamical pattern generation utilizing coexisting periodic grouping states is demonstrated by numerical experiments.

II. ANTIPHASE PERIODIC STATES IN MULTIMODE INTRACAVITY SECOND-HARMONIC-GENERATION LASERS

A. Model equations

The intracavity second-harmonic generation (ISHG) in multimode lasers can be described by the following model equations [5]:

$$\frac{dI_k}{dt}=K\left(G_k-\alpha-g\epsilon I_k-2\epsilon\sum_{j\neq k}\mu_{jk}I_j+s_{i,k}\right)I_k, \qquad (1)$$

$$\frac{dG_k}{dt}=\gamma-\left(1+I_k+\beta\sum_{j\neq k}I_j\right)G_k. \qquad (2)$$

Here, $t=T/\tau$ is the normalized time (τ is the population lifetime), I_k is the intensity for the kth longitudinal mode, G_k is the modal gain associated with the kth mode, $K=\tau/\tau_c$ (τ_c is the cavity round-trip time), α is the cavity loss, γ is the small-signal gain, and β is the cross-saturation parameter among oscillating modes. The term ϵ is the coefficient of nonlinear conversion into the second harmonic and g is a geometrical factor whose value depends on the phase delays of the amplifying and doubling crystals and on the angle between the fast axes of these two crystals. The lasing modes are specified to oscillate in either of two polarizations. $s_{i,k}$ denotes the seeding pulse. In Eq. (1), $\mu_{jk}=g$ if mode j and mode k have the same polarization, while $\mu_{jk}=1-g$ if the two modes have orthogonal polarizations. We have made the simplifying approximation that α, β, γ, and ϵ are the same for all modes. The present model is easily extended to include the globally coupled laser array ISHG model, in which a small-signal gain of each laser element can be controlled [12].

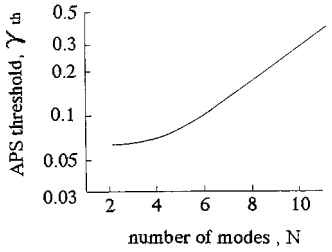

FIG. 1. The threshold small-signal gain for APS γ_{th} as a function of system size N. Adopted parameter values are given in the text.

B. Antiphase periodic state

In the case of relatively small frequency-doubling coefficients, APS's consisting of ''spiking-type'' pulses are born via a Hopf bifurcation [13]. In this case, APS's are destabilized when a small-signal gain (e.g., pump parameter) is increased and local APS chaos appears, leading to global chaos. In local chaos regimes, antiphase relationships among pulsed modes are almost maintained, while modal intensities fluctuate chaotically. When global chaos appears, both modal phases and intensities fluctuate chaotically. In the transition process from local to global APS chaos, chaotic itinerancy takes place and self-induced switching among ruins of coexisting local APS chaotic attractors occurs. The important feature of chaotic itinerancy is that it never occurs by an externally applied random force [9,14].

In the regime of highly efficient conversion into the second harmonic, on the other hand, ''Q-switching-type'' APS's consisting of square-wave pulses have been reported to appear when a pump parameter is increased [15]. There coexist $M_{\text{APS}}=(N-1)!$ equivalent APS attractors in the phase space if we assume that all the modes are oscillating in the same polarization. For brevity, the following studies are carried out in the case where all the modes are oscillating in the same polarization.

The threshold small-signal gain for the onset of APS is depicted in Fig. 1 as a function of number of oscillating modes N. Adopted parameter values are $\alpha=0.02$, $\beta=0.292$, $g=0.5161$, and $\epsilon=0.04$ reported in [15]. In the following simulations, these parameter values are fixed. As the number of modes becomes large, the threshold small-signal gain γ_{th} increases and the APS region decreases as well. This is reasonable since input energy shared by lasing modes decreases and the basin of attraction shrinks as N increases as well. A typical example of Q-switching-type APS's in the case of $N=9$ is shown in Fig. 2(a), where $(N-1)!=40\,320$ equivalent APS's coexist in a high-dimensional phase space. It should be noted that the total output shows rather smooth amplitude oscillations superimposed on a constant dc component (plateau).

C. Global intensity circulation

In Fig. 2(b), we display the global intensity gain circulations relative to mode 1. Here, the global intensity circulation is defined as [11]

$$\Gamma_{ij}=\dot{I}_j\prod_{k\neq j} I_k-\dot{I}_i\prod_{k\neq i} I_k. \tag{3}$$

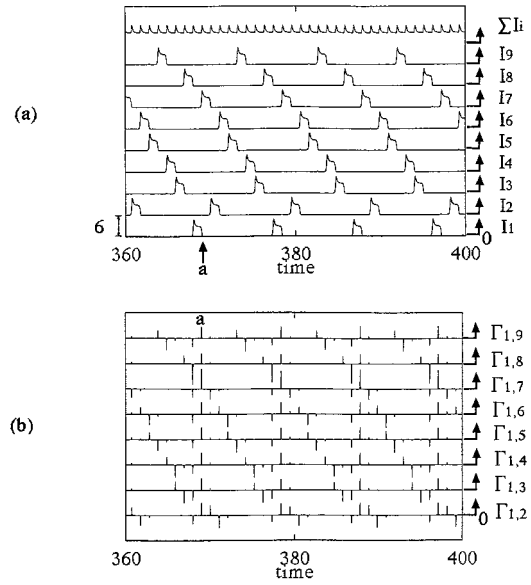

FIG. 2. Antiphase periodic state. $\gamma=0.3$. (a) Temporal evolution of intensities and their summation and (b) corresponding global intensity circulations $\Gamma_{1,j}$.

Here, the overdot denotes the time derivative. The product $\dot{I}_j\Pi_{k\neq j}I_k$ represents the total intensity transfer from all modes to mode j. Γ_{ij} includes the contributions of *all* lasing modes instead of only modes i and j. Hence it describes the global intensity circulation between modes i and j. At the pulse trailing edge $t=a$, a larger intensity (e.g., energy) flow occurs from mode 1 to mode 7 than to other modes. As a result, mode 7 is excited in the next period by obtaining a predominant energy. The same scenario is observed for the energy flows at trailing edges of each mode and the sequence of APS is determined.

III. DYNAMICAL STATES ASSOCIATED WITH APS

In the case of larger system size (e.g., $N\geqslant 8$), various dynamical behaviors, such as clustering, grouping of antiphase motions, and self-induced switching among grouping states, appear in pump regimes below the APS threshold. The result for $N=9$ is summarized in Table I. In this table, CS, GS, and SS denote periodic clustered state, periodic grouping state, and self-induced chaotic switching among grouping states, respectively. In the following, results for $N=9$ are mainly shown. All dynamical states leading to APS's were observed for $N\geqslant 8$ and only SS was observed for N

TABLE I. Dynamical states at different small-signal gains γ. $N=9$.

Small-signal gain γ	Dynamical states
0.12	CS [2,7]
0.125	CS [4,5]
0.151	GS [7,2]
0.17	GS [8,1]
0.20	SS
0.30	APS

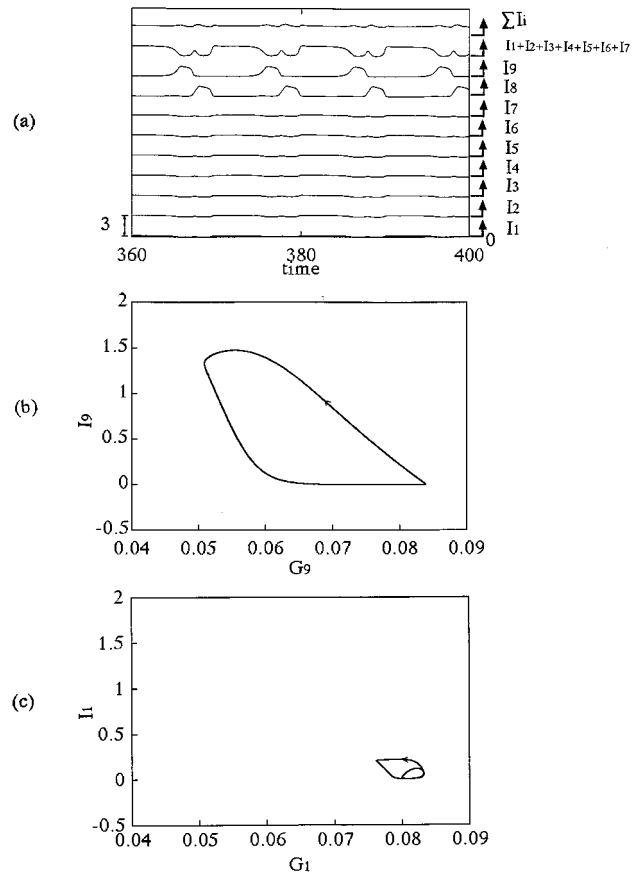

FIG. 3. Temporal evolutions of modal intensities for a clustered state [2,7]. $\gamma=0.12$.

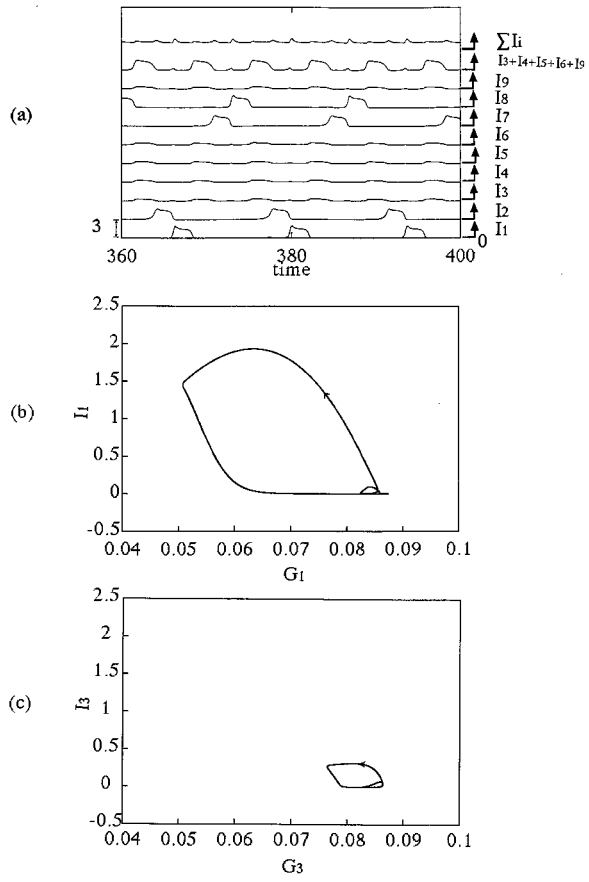

FIG. 4. Temporal evolutions of modal intensities for a clustered state [4,5]. $\gamma=0.125$.

$=6$ and 7. For $N\leqslant 5$, such dynamical states as CS, GS, and SS were not clearly seen. In pump regimes above the APS region, intermittent APS's appear.

A. Clustered state

When a pump parameter is far below the critical pump for the onset of APS, the energy supply to the laser medium is not enough for all the lasing modes to produce APS pulses and clustered states are formed instead. Examples of temporal evolutions of clustered states are shown in Figs. 3 ($[m,n]=[2,7]$) and 4 ([4,5]). In clustered states, m lasing modes emit small-amplitude ''in-phase'' square-wave pulses while other n modes emit larger-amplitude antiphase Q-switched pulses such that the total intensity fluctuates periodically around a larger dc component. In other terms, the sum of in-phase periodic modes is antiphased with Q-switched pulses as shown in Figs. 3(a) and 4(a). The number of in-phase pulses decreases as a pump parameter is increased. A similar clustering behavior is often observed in globally coupled laser systems, and it is referred to as the AD2 state [13].

B. Grouping state

If a pump parameter is increased further, the energy supply to the laser increases accordingly. As a result, the number of Q-switched pulse modes increases. Then, another type of dynamical states of ''grouping'' takes place, in which a group of m modes smaller than N forms complete APS's, while other n modes exhibit higher-frequency periodic sustained relaxation oscillations (abbreviated as SRO) with smaller amplitudes. Therefore the system is grouped into qualitatively different motions with different oscillation time scales. The number of SRO modes decreases as a pump parameter is increased. Examples of temporal evolutions of grouping states and corresponding phase portraits are shown in Figs. 5 ($[m,n]=[7,2]$) and 6 ([8,1]), in which two or one mode(s) exhibit(s) SRO. In this case, there coexist $M_{\mathrm{GS}}=N!(N-n-1)!/n!(N-n)!$ equivalent grouping states in the phase space, where n is the number of SRO modes. Similarly to Fig. 2(a), the system is self-organized such that the total output exhibits rather smooth periodic fluctuations above a dc component, in which the total output oscillation wave form resembles that of SRO.

In this state, nonreciprocal independence of energy flow is found to be established. In short, a unidirectional global intensity flow occurs from the APS mode group to the SRO mode group. The global intensity circulation, which corresponds to Fig. 6(a), is shown in Fig. 7. Mode-to-mode global intensity circulations relative to the SRO mode fluctuate in both directions around zero, however, the sum of global intensity circulation indicates that a cooperative unidirectional energy flow from the APS mode group to the SRO mode is clearly seen to be established. A similar nonreciprocal inde-

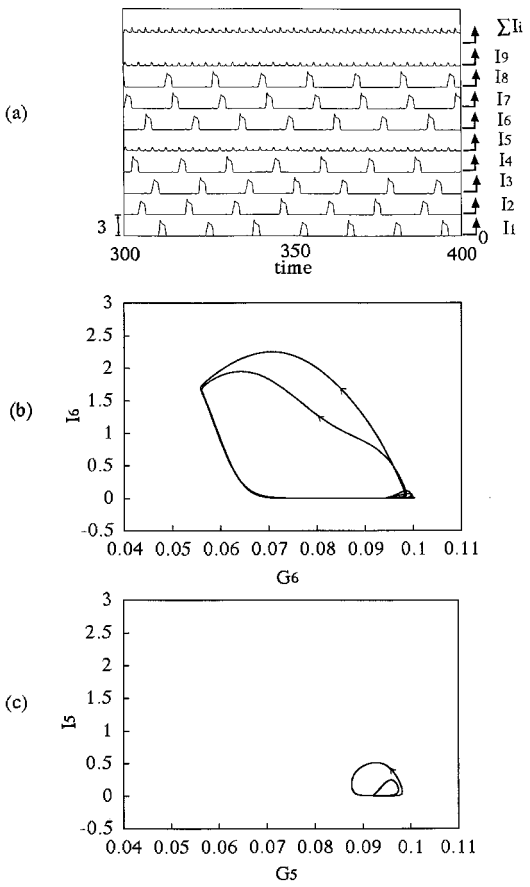

FIG. 5. Grouping state [7,2]. $\gamma=0.151$. (a) Temporal evolution of intensities, (b) and (c) are phase space trajectories.

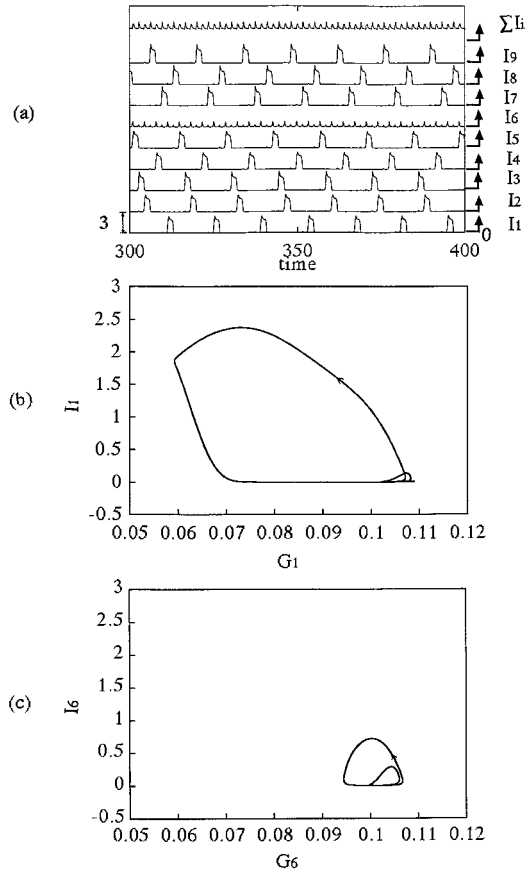

FIG. 6. Grouping state [8,1]. $\gamma=0.17$. (a) Temporal evolution of intensities, (b) and (c) are phase space trajectories.

pendence has also been reported in modulated multimode laser systems [8] and ISHG multimode lasers [15].

C. Self-induced switching among grouping patterns

When a pump parameter approaches the critical pump for the onset of APS, random switching among a factorial number of coexisting grouping states appears. Examples of stochastic switching patterns obtained for different initial conditions are shown in Fig. 8. A calculated Lyapunov spectrum possesses one positive, almost zero Lyapunov exponent (e.g., 0.24, 0.003) and 16 negative ones in the case of Fig. 8. This implies that there is multistability between the M_{GS} number of stable grouping states mentioned in Sec. III B and random switching is occurring between them in this regime, resulting in chaotic motion which possesses at least one positive leading Lyapunov exponent. Depending on initial conditions, various switching patterns are generated after some transients, with different staying periods in the neighborhood of grouping state fixed points. In general, the chaotic SRO motion appears in a different mode at random in time like a ''defect'' wandering over oscillating modes. However, the total intensity still exhibits rather small-amplitude chaotic fluctuations superimposed on a constant dc plateau, similarly to Figs. 5(a) and 6(a). Examples of self-induced switchings obtained for different system sizes are shown in Fig. 9.

There exists such a simple rule that switchings always occur quite ''locally'' featuring an abrupt shift of a defect mode. At the point F in Fig. 8(a), for example, the chaotic SRO mode 7 produces a pulse just after the preceding mode 6, as is indicated by ↑, while mode 8, which was producing pulses after the preceding mode 6 before the switching, switches to a chaotic SRO state in return, as is indicated by ↓. As a result, the SRO mode shifts from 7 to 8 associated with switching. Here, other modes except for the switching pair modes 7 and 8 maintain their APS sequence for *at least more than one APS oscillation period* after the switching. The same switching pattern is established at other switching points in Fig. 8. In some cases, however, successive switchings occur *within one APS oscillation period* obeying the

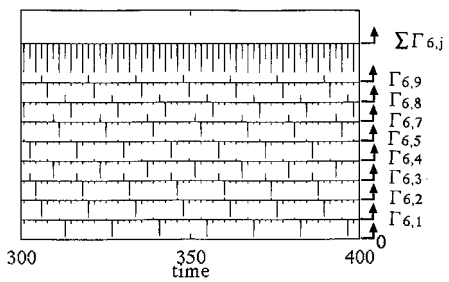

FIG. 7. Unidirectional global intensity flow corresponding to the grouping state [8,1] shown in Fig. 6(a).

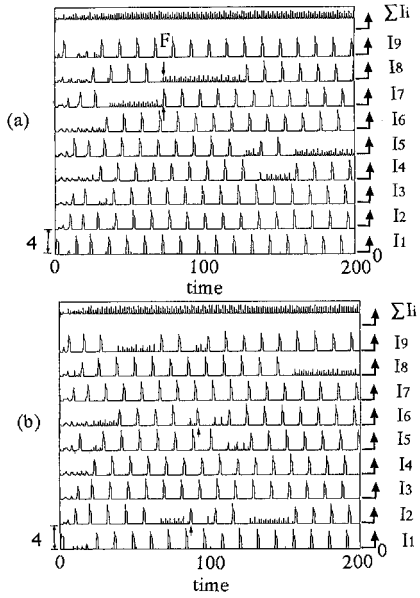

FIG. 8. Self-induced switching states obtained for different initial conditions. $\gamma=0.2$.

above-mentioned rule as indicated by arrows in Fig. 8(b).

A cooperative unidirectional energy flow from the APS mode group to the SRO mode, which was shown in Fig. 7, is found to be occurring even in this chaotic domain. The result is shown in Fig. 10, together with corresponding temporal intensity evolution, where the sequences of APS before and after the switching point S are depicted by numbers. At the switching point, the global intensity flow in the system changes abruptly.

A clear theoretical explanation for the self-induced switching in this high-dimensional system has yet to be known; however, we shall characterize dynamics occurring

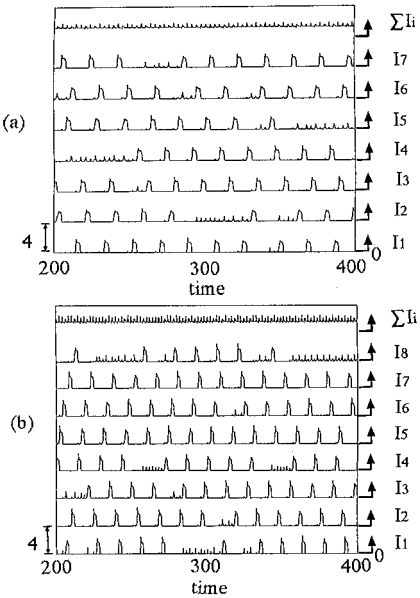

FIG. 9. Self-induced switching obtained for different system sizes. (a) $N=7$, $\gamma=0.11$. (b) $N=8$, $\gamma=0.15$.

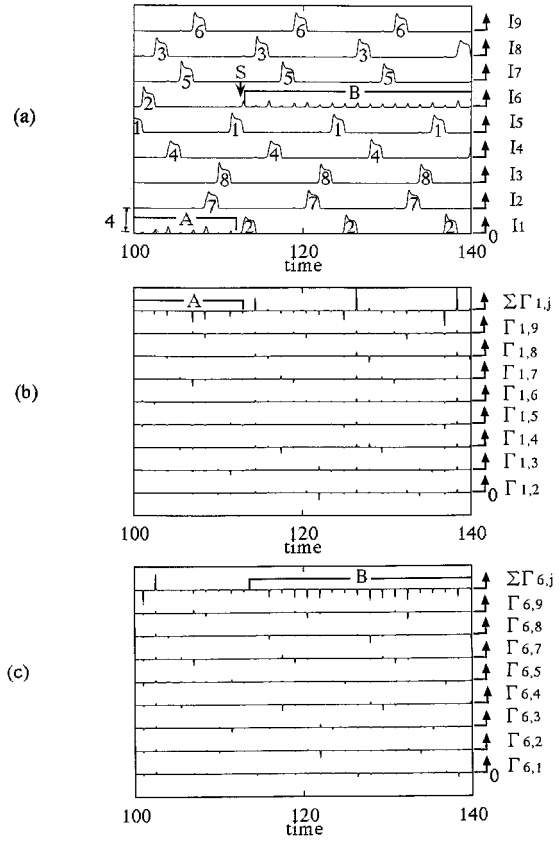

FIG. 10. Dynamical characterization of self-induced switching. $\gamma=0.2$. (a) Temporal evolution of intensities, where the switching sequence is indicated by numbers. (b) Global intensity circulation $\Gamma_{1,j}$ before the switching. (c) Global intensity circulation $\Gamma_{6,j}$ after the switching.

near the switching point to identify the switching mechanism numerically. For this purpose, global intensity circulations between the preceding chaotic APS mode 5 to the switching pair modes 1 and 6, and their difference are shown in Fig. 11. From this figure, it is found that a slightly larger energy flow to mode 1 just before switching point S indicated by $\uparrow$ prefers the excitation of mode 1 rather than mode 6. Accordingly, mode 1 produces an APS pulse, while mode 6 switches to the chaotic SRO state in return. Additionally, energy flows from the preceding APS mode 5 to other modes,

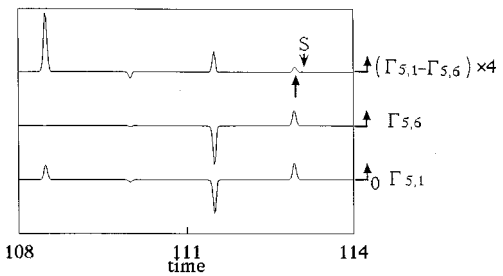

FIG. 11. Global intensity circulations near the switching point in Fig. 10, involving the preceding mode 5 and switching pair modes 1 and 6.

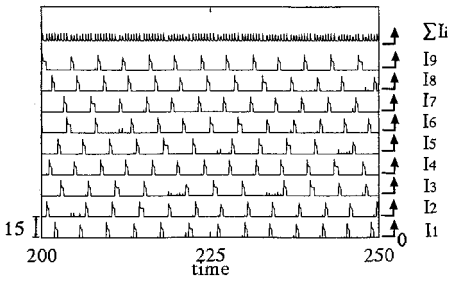

FIG. 12. Intermittent chaotic antiphase state. $\gamma=1$.

except for the switching pair modes, are found to be uniform and much smaller than to mode 1. This parallels the APS pulse excitation mechanism in terms of energy flow shown in Fig. 2(b).

It should be stressed that local chaos, which is to be born from each periodic grouping state, is absent in this model. In modulated multimode lasers, on the contrary, local grouping chaos exists and a transient chaotic itinerancy among the ruins of local grouping chaos attractors terminated by a clustered state is demonstrated [8]. The absence of localized chaos born from periodic grouping states may suggest that self-induced switching in the present system may be interpreted in a different context. This point will be discussed later.

D. Intermittent chaotic antiphase state

If a pump parameter is increased up to a critical point, all the lasing modes can share enough pump energy (e.g., population inversion) equivalently and realistic APS as in Fig. 2(a) is established. As a pump parameter is increased above the APS region, APS pulses of individual modes exhibit intermittent destabilization as shown in Fig. 12. A calculated Lyapunov spectrum possesses three positive leading Lyapunov exponents, indicating hyper-chaos. It is interesting to note that the present dynamical state is qualitatively different from other states in the sense that individual modes produce APS pulses with different shapes in time, whereas the total intensity exhibits intermittent spikes superimposed on a dc component.

Finally, it should be pointed out that the total output always exhibits rather smooth amplitude variations about 15–20 % above a large dc component, while individual modes show a violent self-organized pulsation such that the laser produces more stable total output.

IV. PERTURBATION-INDUCED SWITCHING-PATH FORMATION AND CONTROLLED DYNAMIC PATTERN GENERATION

A. Switching-path formation by perturbation to SRO mode

There may exist a huge number of switching paths connecting different grouping states. The self-induced cooperative dominant energy flow to the chaotic SRO mode from the preceding APS pulse resulting in switching, which is identified in the preceding section, suggests the possibility of controlled switching among grouping states by an external

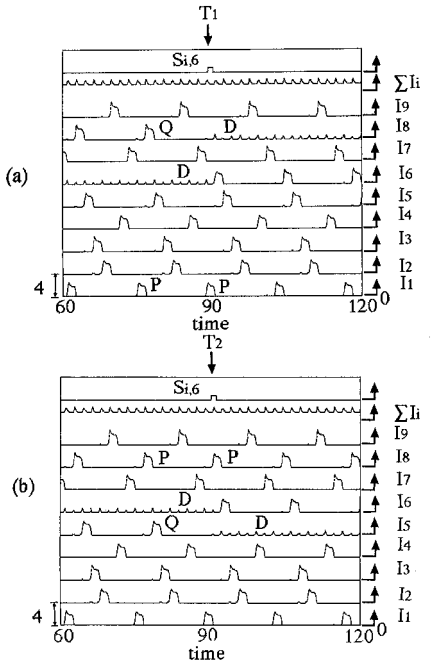

FIG. 13. Perturbation-induced switching among periodic grouping states. $\gamma=0.17$. The perturbation pulse intensity $s_{i,k}=0.002$ and pulse width $\Delta t=1$.

physical manipulation. In order to check the idea of ''multiple'' connections between coexisting grouping states and controlled switching, we apply an extremely weak light pulse, which is three orders of magnitude smaller than the APS pulse height (i.e., $s_{i,k}\geqslant 0.002$, where pulse width $\Delta t=1$), to a chaotic SRO mode as an ''external'' perturbation instead of ''self-induced'' dominant energy flow to a SRO mode and control the energy flows (e.g., switching-path formation) in regimes of *periodic* grouping states. From repeated numerical experiments, the following empirical rule is obtained.

Rule. Assume an APS mode sequence $\{\ldots,P,Q,\ldots\}$, where P and Q are arbitrary modes. If a perturbation pulse is applied to the SRO mode D at the time of leading edge of an APS pulse of the Pth mode, the SRO mode D emits an APS pulse after the preceding Pth mode instead of the Qth mode and the Qth mode switches to the SRO state in return, in which other modes maintain their APS sequence.

Results of a light-injection-induced switching experiment are shown in Fig. 13, where a light pulse with the same energy is applied to the periodic SRO mode 6 at T_1 (leading edge of the mode 7 pulse) and T_2 (leading edge of the mode 1 pulse), starting from the same initial condition. After a time delay on the order of the APS pulse period, the SRO mode produces APS pulses, while mode 8 [see Fig. 13(a)] or mode 5 [see Fig. 13(b)] switches to a SRO state in return, depending on the timing of the applied perturbation. As is stated in the rule, such switchings occur quite locally and other modes except for switching pair modes [e.g., mode 6 and mode 8 in Fig. 13(a), mode 6 and mode 5 in Fig. 13(b)] maintain their APS sequence similarly to self-induced switchings shown in Fig. 8. This implies that $N-1$ different

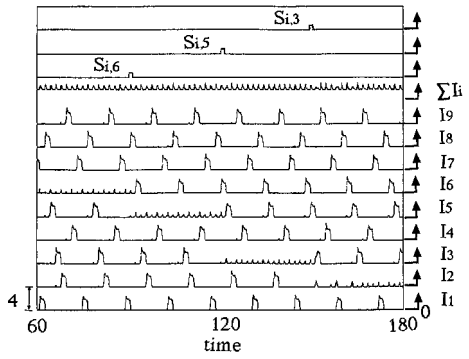

FIG. 14. Successive generation of different periodic grouping states. $\gamma=0.17$. $s_{i,k}=0.002$, $\Delta t=1$.

switching paths can be selectively created by changing the timing of the applied perturbation to the SRO mode within one APS oscillation, starting from the same grouping state. Note that such switchings do not occur if one applies ''uniform'' perturbation pulses to all the lasing modes simultaneously.

When a timing of perturbation is shifted from the leading edge and/or a pulse intensity is too strong, successive switchings indicated by arrows in Fig. 8(b) take place *within one APS oscillation period*, and finally an unexpected periodic GS pattern appears. In this case, externally applied switching pulses act like random perturbations and one cannot predict a new pattern according to the above-mentioned rule.

B. Controlled successive generation of factorial dynamic patterns

If the initial periodic GS pattern is given, one can generate desired periodic GS patterns successively in a controlled manner by successive applications of switching pulses to SRO modes at different times according to the ''program,'' which is based on the above-mentioned switching rule. In short, extremely flexible successive excitations of a factorial number of dynamic patterns with weak perturbation signals is possible in the present system by a systematic physical manipulation based on the rule mentioned above. In the case of $N=10$, for example, the maximum number of available patterns is $M_{\mathrm{GS}}=403\,200$. An example of successive generations of periodic GS patterns is shown in Fig. 14. In this example, the periodic GS pattern changes its APS sequence as $\{1,8,5,3,2,9,4,7\}\rightarrow\{1,8,6,3,2,9,4,7\}\rightarrow\{1,8,6,5,2,9,4,7\}\rightarrow\{1,8,6,5,3,9,4,7\}$ in accordance with the sequential shift of the ''defect'' mode $6\rightarrow5\rightarrow3\rightarrow2$. Random switchings are occurring when perturbation pulses with different intensities and phases are applied to individual modes at random. In chaotic itinerancy systems, random switching among different attractors never occurs when a random external noise is applied [9,14].

If one tries to realize the ''target'' periodic GS pattern starting from a particular initial periodic GS pattern which has a large norm (distance) from the target pattern, there exist many switching routes reaching the target pattern via different intermediate GS patterns. Then, an interesting question arises as to how to find the easiest switching route to reach the target pattern with the minimum number of perturbation signals.

The originality of this perturbation-induced switching is that the present autonomous antiphase dynamical system changes its dynamical pattern *by recognizing the ''timing''* of an externally applied weak perturbation.

V. SUMMARY AND DISCUSSION

In summary, the formation process of antiphase periodic states is investigated numerically in the reference model of multimode intracavity second-harmonic lasers. Various dynamical states associated with antiphase periodic states, such as clustered state, grouping state, self-induced switching state among coexisting grouping states, and intermittent chaotic antiphase state have been found.

Dynamical characterization of grouping states has been carried out in terms of the global intensity circulation concept. Nonreciprocal independence of intensity flow in grouping states as well as cooperative selective intensity flow responsible for self-induced switching among grouping states have been identified.

A clear understanding of peculiar self-induced switchings among coexisting grouping states has yet to be known theoretically, however, we try to give one of the plausible phenomenological explanations for the occurrence of self-induced switchings. The remarkable point of the present self-induced switching is the one-to-one correspondence between the occurrence of chaos and random switchings. This may suggest the possible existence of ''heteroclinic'' connections between coexisting grouping states. In other terms, an unstable manifold originating from one grouping state (e.g., saddle) is considered to cross a stable manifold of one of the other grouping states. If such a crossing occurs transversally, it is known that the system switches between coexisting fixed points (e.g., grouping states) at random, at the same time, motion around grouping states exhibits very complex chaotic behavior.

The timing-controlled switching-path formations among periodic grouping states and successive generations of different dynamic patterns by externally applied perturbation signals have been demonstrated by numerical experiments. In the case of self-induced switching, a perturbation force is self-generated chaotically and a random switching takes place. The important message concerning switching behaviors is that the present system changes it dynamical pattern by recognizing the ''timing'' of perturbations.

Finally, it is worth mentioning that in the present reference model system, APS patterns survive stably for a large system size as compared with other systems exhibiting APS. This implies that rewritable factorial dynamic pattern memory with an extremely large capacity of $C=\log(N-1)!/\log 2$ (in bits) is feasible if a direct assignment to desired dynamical patterns by the injection-seeding method proposed in [5,6,11] is applied.

[1] P. Hadley and M. R. Beasley, Appl. Phys. Lett. **50**, 621 (1987).
[2] K. Yoshimoto, K. Yoshikawa, Y. Mori, and I. Hanazaki, Chem. Phys. Lett. **189**, 18 (1992).
[3] M. Yoshimoto, K. Yoshikawa, and Y. Mori, Phys. Rev. E **47**, 864 (1993).
[4] T. Baer, J. Opt. Soc. Am. B **3**, 1175 (1986); K. Wiesenfeld, C. Bracikowski, G. James, and R. Roy, Phys. Rev. Lett. **65**, 1749 (1990).
[5] K. Kubodera and K. Otsuka, IEEE J. Quantum Electron. **QE-17**, 1139 (1981); K. Otsuka, Phys. Rev. Lett. **67**, 1090 (1991).
[6] K. Otsuka and J.-L. Chern, Phys. Rev. A **45**, 8288 (1992).
[7] W. J. Freeman and C. A. Skarda, Brain Res. Rev. **10**, 147 (1985).
[8] K. Otsuka, Y. Sato, and J.-L. Chern, Phys. Rev. A **54**, 4464 (1996).
[9] K. Otsuka, T. Nakamura, J.-Y. Wang, and J.-L. Chern, Quantum Semiclassic. Opt. **8**, 1179 (1996).
[10] K. Otsuka and Y. Aizawa, Phys. Rev. Lett. **72**, 2701 (1994).
[11] K. Otsuka, J.-Y. Wang, P. Mandel, and T. Erneux, Quantum Semiclassic. Opt. **7**, 461 (1995).
[12] P. Mandel, J.-Y. Wang, and K. Otsuka, Quantum Semiclassic. Opt. **8**, 399 (1996).
[13] J.-Y. Wang, P. Mandel, and T. Erneux, Quantum Semiclassic. Opt. **7**, 169 (1995).
[14] K. Ikeda, K. Otsuka, and K. Matsumoto, Prog. Theor. Phys. Suppl. **99**, 295 (1989).
[15] P. Mandel and J.-Y. Wang, Opt. Lett. **19**, 533 (1994).